DETECTION OF DELAMINATIONS IN 5-HARNESS SATIN GFRP EPOXY LAMINATES USING DIC

O. Z. Ajmal[1], A. D. Crocombe[1], M. R. L. Gower[2], D. A. Jesson[1], S. L. Ogin[1]

[1]Centre for Engineering Materials, Department of Mechanical Engineering Sciences,
Faculty of Engineering and Physical Sciences, University of Surrey, Guildford, UK
Email: o.ajmal@surrey.ac.uk; a.crocombe@surrey.ac.uk; d.jesson@surrey.ac.uk; s.ogin@surrey.ac.uk
Web page: http://www.surrey.ac.uk/mes/index.htm
[2]National Physical Laboratory, Hampton Road, Teddington, Middlesex, UK
Email: michael.gower@npl.co.uk
Web page: http://www.npl.co.uk/people/michael-gower

Keywords: Defects, Damage, Fatigue behaviour, Quasi-static testing

Abstract

Digital Image Correlation (DIC) can be used to obtain full-field strain information of specimens under load. Through analysis of the resultant strain-contours, defects such as delaminations in composite materials can be detected based on their effect on the deformation behaviour. This paper focuses on the use of DIC to detect the presence of fully embedded artificial delaminations, introduced during the manufacturing process, inside a flat panel specimen under three-point bending. Two types of delamination insert have been considered: an insert containing two sealed pieces of PTFE, and an insert consisting of a single sheet of PTFE in combination with a stress-raiser. When tested in three-point bending, the position and approximate size of the delaminations were clearly visible due to the presence of a plateaux in the longitudinal surface strain profile. Finite element modelling predictions were in good agreement with the DIC measurements for both types of artificial delamination.

1. Introduction

As the range of composite material applications grows, so it becomes increasingly necessary to develop non-destructive testing (NDT) techniques which can be easily and rapidly deployed, and which can provide useful and accurate information on the current damage state of a composite component/structure. Current NDT techniques of interest include ultrasonic inspection techniques[1], acoustography [2], radiographic inspection [3], as well as shearography and active thermography [4]. Recently, the rapid improvement in the ready applicability of the DIC technique suggests that DIC may also be a candidate as an NDT technique [5–7]. The present work is a part of an ongoing project concerned with determining the accuracy and resolution of the DIC technique when used to monitor the growth of delaminations.

In the work described in this paper, a 3D DIC system has been used to detect and monitor delaminations in a quasi-isotropic glass fibre-reinforced plastic (GFRP) laminate and in a cross-ply GFRP laminate, both fabricated using 5-harness satin weave (5-HSW) fabric and epoxy resin. Two types of artificial delamination have been used. The first consisted of thin polytetrafluoroethylene (PTFE) sheets combined with Flashbreaker®2 tape embedded within a quasi-isotropic laminate [8]; it proved impossible to grow this delamination in fatigue, as expected (see below). The second artificial delamination consisted of a single sheet of PTFE in a cross-ply laminate (again using 5-HSW fabric), this time combined with a stress-raiser in the form of a cut in the surface ply fabric; this configuration facilitated delamination growth (over the PTFE insert) in fatigue. The DIC experimental results for both types of artificial delamination are compared to Finite Element (FE) model predictions of the surface strains.

Excerpt from ISBN 978-3-00-053387-7

2. Experimental Methods

As mentioned above, two types of delamination were tested. The first type of artificial delamination was manufactured using two square pieces of 0.05 mm thick PTFE film (Goodfellow Ltd), surrounded and encompassed by two larger pieces of Flashbreaker® 2 tape, as shown schematically in Figure 1. This type of insert has dimensions of 32 x 32 mm and a thickness of 0.23 mm. This arrangement ensured that the two surfaces of the PTFE film in contact were free to slide relative to each other, producing an artificial delamination with extremely low friction between the PTFE surfaces. This type of artificial delamination has been used in previous work to optimise the use of ultrasonic C-scan as an NDT technique [8]. The delamination was then introduced between the first and second plies of a 16 ply GFRP composite $[(0/90)/\pm45]_{4S}$ manufactured using 5-HSW fabric (supplied by Fothergill Engineered Fabrics Ltd), infused with an epoxy resin consisting of Epoxide 300 resin, MNA hardener and Ancamine. Laminates with dimensions of 300 x 300 x 4.75 mm with embedded delaminations, were manufactured using a (wet) hand lay-up technique, as described in [9]. The similarity in the refractive indices of the glass and epoxy resin produces transparent laminates.

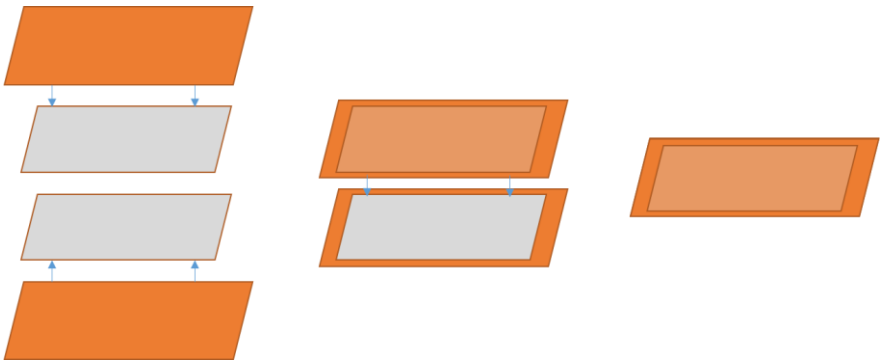

Figure 1. Manufacturing method of the pocket delamination inserts. (a) Two square pieces of PTFE and two larger squares of Flashbreaker®2 tape. (b) The PTFE is adhered to the tape such that there is still about 1-2 mm of tape visible at each edge. (c) Both pieces of PTFE/Flashbreaker®2 tape were superimposed and the edges of the tape were brought together, sealing the 2 sheets of PTFE.

The second type of artificial delamination consisted of a single square film of 0.05 mm thick PTFE with dimensions of 25.4 x 25.4 mm. As the purpose of this type of insert was to grow a delamination, the ply above the insert was cut before the infusion of resin to provide a stress-raiser. The lay-up of the composite panel was changed for these experiments to a cross-ply configuration $[(0/90)]_{8S}$, but otherwise specimens containing this type of delamination were produced in the same way as the first type of delamination. During the addition of the resin in the hand lay-up technique, the inserts frequently shift slightly, causing the cuts in the fabric not to lie perfectly across the centre of the inserts.

Specimens cut from the laminates had dimensions of 265 x 70 x 4.75 mm. The specimens were tested in three-point bending under quasi-static loading, with the support rollers 200 mm apart. The DIC system was set up to observe the compressive surface between rollers 1 and 2 (see Figure 2). To monitor the tensile surface, the specimen was turned upside down and viewed from the other face; in this case, the DIC system was set up to observe the specimen between rollers 1 and 3. Figure 2 shows a schematic of a specimen in the three-point bend arrangement. The orange squares represent the location of the embedded delaminations which have dimensions of 32 mm x 32 mm. For the fatigue growth of the second type of artificial delamination, the specimens were cycled between 60 and 600 N (approximately 6 – 60 % of the quasi-static failure load) at a frequency of 2 Hz, using an Instron 8511 with a 5000 lb (22.2 kN) loadcell.

Excerpt from ISBN 978-3-00-053387-7

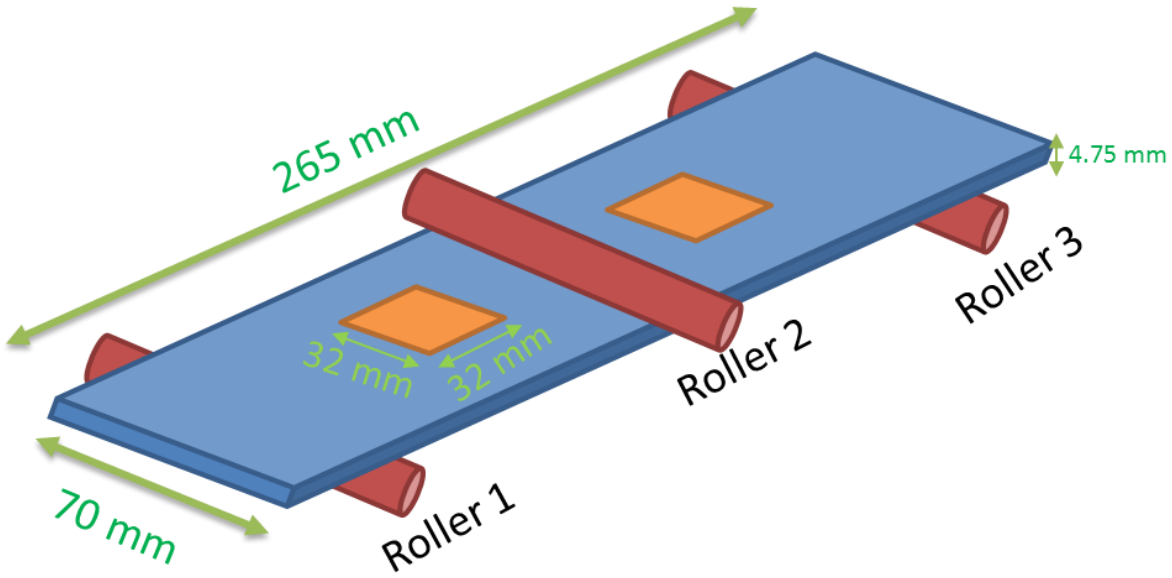

Figure 2. Schematic of a test specimen under 3 point bending loading with the position of the embedded delaminations highlighted in orange.

The DIC system consisted of two 9 megapixel Allied Vision Technology Manta cameras, with LINOS MeVis-C 35 mm f/1.6 lenses. Each camera contains a 2/3" (16.9 mm) chip. The apparatus was supplied by Correlated Solutions Inc. When obtaining DIC results, the specimens were placed in an Instron 1185 with a 10 kN loadcell and loaded to a 4 mm displacement (~220 N for the $[(0/90)/\pm45]_{4S}$ specimens and ~315 N for the $[(0/90)]_{8S}$ specimens) at a rate of 2 mm/min. The cameras were placed above the specimen to monitor the specimen between rollers 1 and 2, and below the specimen to monitor the specimen between rollers 1 and 3. For this work, the combination of the DIC cameras and testing machine required that the DIC images were not taken perpendicular to the specimen surface. The subset grid for the DIC results was specified at 27 x 27 pixels and a step size of 7 for each set of results.

3. Finite Element Modelling

FE models were created to represent the experimental specimens under their respective loads. The FE analysis was undertaken in 3D, using the software Abaqus/Standard version 6.14. The geometries and dimensions were based on the experimental specimens, as shown in Figure 2; as mentioned above, due to the nature of the manufacturing technique, which caused the inserts to shift during laminate fabrication, the position of the inserts in the model were modified to match each of the specimens tested. The models all used eight noded brick elements with reduced integration and hourglass control. The plies were one element thick, and the in-plane dimensions of the elements were 2 mm x 2 mm. The support rollers were represented by fixing the displacement of an appropriate line of nodes across the specimen in the through-thickness direction. A through-thickness load was applied to the appropriate line of nodes across the width of the specimen top surface using a coupling constraint. Each ply was assigned the properties given in Table 1, taken from [10].

Excerpt from ISBN 978-3-00-053387-7

Table 1. GFRP ply properties used for FE modelling [10]

Parameter	Value
E_1 (GPa)	21
E_2 (GPa)	21
E_3 (GPa)	8.55
v_{12}	0.183
v_{13}	0.0305
v_{23}	0.075
G_{12} (GPa)	3.7
G_{13} (GPa)	3.5
G_{23} (GPa)	3.5

The first type of inserts were modelled by partitioning the plies and assigning the material properties of the PTFE and Flashbreaker®2 tape, as shown in Table 2, to the areas in which the inserts were located. For the PTFE-only specimens, the models also included a partition in the top plies through the width of the specimen above the insert. In all of the models, every ply was tied to the adjacent plies in the laminate apart from the area over which the delamination insert was present. This partition was assigned the properties of the epoxy resin to represent the resin-rich region caused by cutting the top ply (to create the stress raiser) during the manufacturing; measurements suggested the resin-rich region was approximately 2 mm thick above the centre of the insert, so this distance was assumed in the model.

Table 2. Material properties of the epoxy resin and PTFE used for FE modelling

	Parameter	Value
Epoxy Resin	*E* (GPa)	3.8
	v	0.37
PTFE/ Tape	*E* (GPa)	0.8
	v	0.48

4. Results

4.1 Introduction

In this section, results will be presented first for the PTFE/Flashbreaker®2 artificial delamination, with the DIC measurements of strain compared to FE predictions. These are followed by the results for the single sheet of PTFE delamination.

4.2 PTFE/Flashbreaker®2 tape delaminations

As described above, this artificial delamination was located between the first and second plies of the 16-ply laminate. Quasi-static three-point bend testing was carried out as described in Section 2, with the delaminations located near the compressive face. Figure 3(a) shows the longitudinal compressive surface strains at an applied load of 220 N, which was 20% of the static failure load of the laminate in three-point bending. The actual location of the defect is indicated by the dashed lines in the figure; the edge of the defect closest to roller 1 is at a distance of about 66 mm from the end of the specimen. Figure 3(b) shows the longitudinal surface strains as indicated by the DIC measurements when progressing from the left-hand edge of the specimen, past roller 1 and towards roller 2; the line

Excerpt from ISBN 978-3-00-053387-7

traversed is shown by the black line in Figure 3(a). At the edge of the specimen, beyond roller 1, the DIC shows a strain of approximately zero (as would be expected). Between roller 1 and the edge of the delamination, the strain becomes increasingly negative until a plateaux is reached at about 66 mm from the end of the coupon - i.e. at a location corresponding to the edge of the delamination. From this point, for a distance of about 32 mm, the compressive strain remains constant. Figure 3(b) shows that similar results are predicted by the FE modelling with the plateaux in the compressive strain values corresponding approximately, in magnitude and extent, to the experimental measurements. It is clear that the defect shape and size can be reasonably well quantified and the agreement between the DIC and the FE results is good.

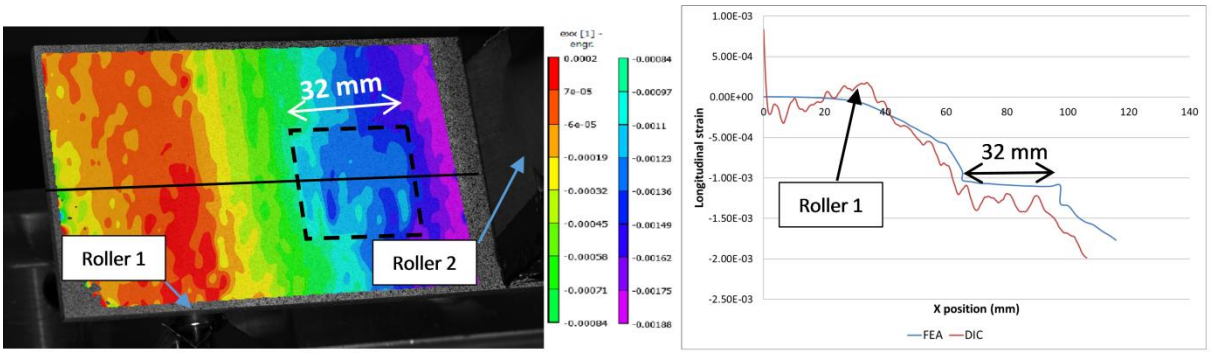

(a) *(b)*

Figure 3. Experimental results from a three point bend test of a 5-HSW laminate specimen with a square-shaped PTFE/Flashbreaker®2 tape artificial delamination in 3-point bending at an applied load of 220 N: (a) DIC Longitudinal strain contours, the dotted line shows the location of the delamination and the solid line is the line along which the surface strains have been compared (i.e. experimental results and FE modelling); (b) Comparison of longitudinal strains from the FEA and DIC results, taken along the longitudinal mid-span of the specimen as indicated by the solid line in (a).

Subsequent tests under both quasi-static and fatigue loading failed to grow the delamination. For example, the quasi-static load was increased at a rate of 2 mm/min in an attempt to grow the delamination but local buckling on the surface above the defect occurred before the delamination grew. Fatigue loading with a peak load of 70% of the quasi-static failure load for 50,000 cycles also failed to produce any delamination growth.
Figure 4 shows the local buckling which occurred at a load of 741.3 N and is clearly observable in the DIC results as a region of greatly enhanced surface strain in the compressive strains.

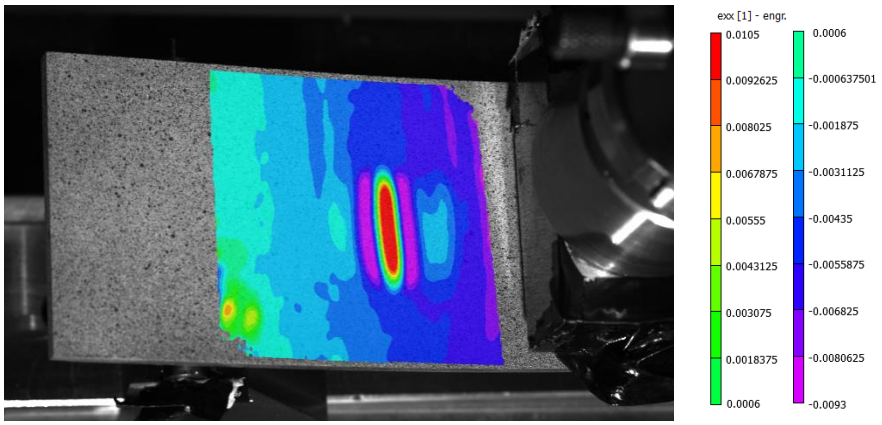

Figure 4. Region of high strain where local buckling has occurred at a load of 741.3 N

Excerpt from ISBN 978-3-00-053387-7

4.3 PTFE/stress raiser delamination

As the PTFE/Flashbreaker®2 artificial delaminations could not be grown under quasi-static or fatigue loading, a second type of defect was developed. In this case, a single layer of PTFE was used, with the addition of a stress-raiser in the form of a cut introduced into the top layer of the glass fabric prior to manufacturing the laminate. For tests with this type of artificial delamination, the coupons were tested with the delamination near to the tensile face of the laminate. It was suspected that a thin PTFE layer by itself would not produce a delamination due to the likelihood of the epoxy bonding to the PTFE during manufacture. This bond, while weaker than the bond between the laminate layers, still transfers load. However, it was anticipated that the cut in the fabric, creating a stress-raiser, would facilitate failure of the bond between the PTFE and the top layer of the laminate, thus creating a well defined delamination growth.

Specimens with the second type of artificial delamination were subjected to cyclic loading with a peak load of 600 N (R = 0.1) at 2 Hz for 10,000 cycles. Figure 5(a) shows an image of the PTFE artificial delamination in the transparent laminate before fatigue loading, with the specimen under a load of 315 N. The DIC image shows an increase in the longitudinal tensile surface strains. The variation in strain along the coupon for these "pre-fatigue" results are shown in Figure 6. The strain increases linearly from about 500 με near to roller 1, to about 2,800 με at the centre of the coupon; the mirror-image of this strain distribution occurs for the other half of the specimen. At the location of the cut in the top layer of the fabric there is a small perturbation in the strain for both halves of the coupon.

With this PTFE/stress-raiser insert, it proved possible to grow the delamination under fatigue loading. Figure 5(b) shows the appearance of the delamination after 10,000 fatigue cycles. The delamination initiated at the location of the cut in the fabric and grew at the interface between the PTFE layer and the top layer of the laminate. Interestingly, the delamination does not extend beyond the limits of the PTFE insert. Figure 5(b) also shows the DIC image at a load of 315 N, and the surface strains derived from the DIC results for this "post-fatigue" delamination are shown in Figure 6.

As before, the overall changes in the strains shown in Figure 6 correspond to what would be expected for the surface strains in a three-point bend test. However, there are two significant changes. First, there are now large perturbations at the locations of the cuts in the surface fabric of the laminate and, second, there are strain plateaux (i.e. regions of constant strain) which occur in the vicinity of the delamination. These plateaux correspond to the plateaux seen for the PTFE/Flashbreaker®2 results of Figure 3(b). Consequently, it can be concluded that the delaminations growing from the PTFE/stress-raiser act as real delaminations, producing the same effects on the surface strains as the PTFE/Flashbreaker®2 delaminations, with the added advantage that this second type of artificial delamination grows under fatigue loading. The FE predictions of the surface strains for the PTFE/stress-raiser artificial delaminations are also shown in Figure 6, where again the plateaux in the strain values adjacent to the delaminated areas can be seen, in addition to the large perturbations due to the cut in the surface fabric. The artificial delamination shown in Figure 5 corresponds to the right-hand side of the strain results and predictions in Figure 6.

Prior to fatigue loading, the insert was fully bonded to the surrounding epoxy and the presence of the PTFE insert could, therefore, not be detected using DIC. However, once the insert de-bonds from the epoxy due to the fatigue loading, load transfer to the delaminated surface ply is no longer possible and the surface ply above the defect remains at a constant level of strain, thus producing the plateaux observed in the strain profiles This is the same mechanism for the strain plateaux observed with the PTFE/Flashbreaker®2 inserts. The spike in strain where the fabric was cut is probably due to the higher deformations within this resin-rich region.

Excerpt from ISBN 978-3-00-053387-7

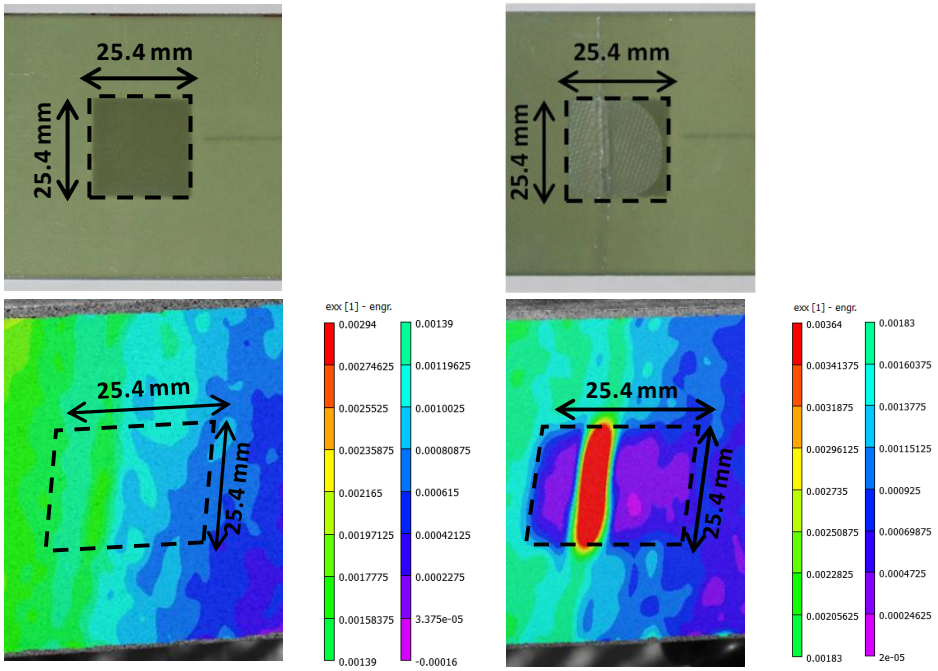

(a) *(b)*

Figure 5. Images of the surfaces directly above a typical specimen with a PTFE insert and a cut fabric (a) pre-fatigue and (b) post fatigue. [Note that the shape of the square PTFE insert appears distorted in the lower figures since the DIC images were not taken perpendicular to the specimen surface.]

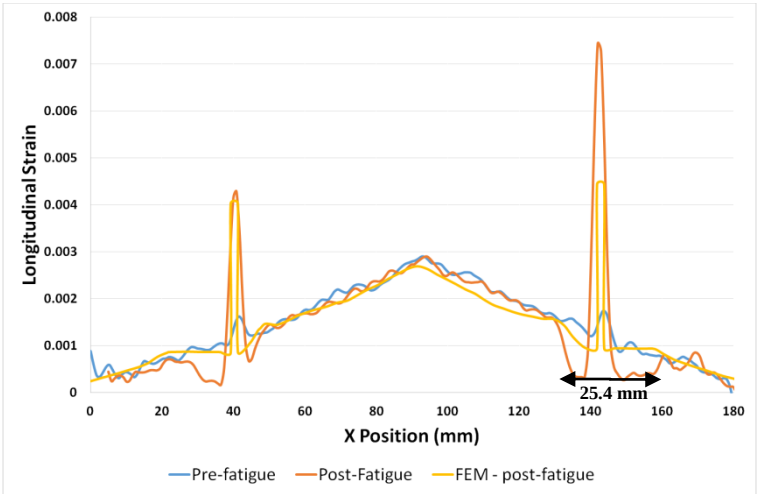

Figure 6. Comparison of DIC longitudinal strains along the centre line of the specimen with the PTFE/stress-raiser artificial delamination both before and after the growth of the delamination ("pre-fatigue" and "post-fatigue"); FEA strain predictions after the growth of the delamination ("FEM - post-fatigue") are also shown.

5. Conclusions

This work has investigated the possibility of determining the location and size of embedded artificial delaminations using the DIC technique. Two types of artificial delamination have been investigated: (i) PTFE/Flashbreaker®2, and (ii) a single layer of PTFE in combination with a stress-raiser.
Specimens containing PTFE/Flashbreaker®2 artificial delaminations demonstrated the ability of the

Excerpt from ISBN 978-3-00-053387-7

DIC to locate the position and extent of the artificial delamination. With the specimens tested under three-point bending, a plateaux occurred in the strain distribution corresponding to the position and extent of the delaminations; the plateaux is a consequence of the constant stress carried by the (delaminated) outer ply of the composite.

To facilitate further work on the accuracy and resolution of the DIC technique for monitoring the growth of delaminations, a second type of artificial delamination has been developed consisting of a single sheet of PTFE and a stress-raiser in the form of an adjacent cut ply. Due to the bond between the PTFE and the epoxy resin, the PTFE insert by itself did *not* behave as a delamination. However, under cyclic loading, a real delamination developed at the PTFE/surface ply interface, initiated through interaction with the stress raiser. The strain changes associated with the PTFE/stress-raiser delamination were in good agreement with FE predictions. In addition, the characteristic plateaux in the strain profile, seen initially with the PTFE/Flashbreaker®2 artificial delamination, was also reproduced.

Acknowledgments

The authors would like to thank Mr. M. Poole and Mr. P. Haynes for assistance with aspects of the experimental work.

References

[1] B. W. Drinkwater and P. D. Wilcox, “Ultrasonic arrays for non-destructive evaluation: A review,” *NDT E Int.*, vol. 39, no. 7, pp. 525–541, 2006.

[2] A. S. Chen, D. P. Almond, and B. Harris, “Impact damage growth in composites under fatigue conditions monitored by acoustography,” *Int. J. Fatigue*, vol. 24, no. 2–4, pp. 257–261, 2002.

[3] K. H. Kim, R. T. Klann, and B. B. Raju, “Fast neutron radiography for composite materials evaluation and testing,” *Nucl. Instruments Methods Phys. Res. Sect. A Accel. Spectrometers, Detect. Assoc. Equip.*, vol. 422, no. 1–3, pp. 929–932, 1999.

[4] Y. Y. Hung, Y. S. Chen, S. P. Ng, L. Liu, Y. H. Huang, B. L. Luk, R. W. L. Ip, C. M. L. Wu, and P. S. Chung, “Review and comparison of shearography and active thermography for nondestructive evaluation,” *Mater. Sci. Eng. R Reports*, vol. 64, no. 5–6, pp. 73–112, 2009.

[5] E. Schwartz, R. Saralaya, J. Cuadra, K. Hazeli, P. A. Vanniamparambil, R. Carmi, I. Bartoli, and A. Kontsos, “The use of digital image correlation for non-destructive and multi-scale damage quantification,” *Proc. SPIE - Int. Soc. Opt. Eng.*, vol. 8692, p. 86922H, 2013.

[6] H. S. Huang, “Non-destructive evaluation by 3D digital image correlation method,” *AIP Conf. Proc.*, vol. 1650, no. 2015, pp. 1343–1349, 2015.

[7] N. Schorer and M. G. R. Sause, “Identification of Failure Mechanisms in Cfrp Laminates Using 3D Digital Image Correlation,” in *Proceedings of the 20th International Conference on Composite Materials ICCM-20, Copenhagen, Denmark*, 2015, no. July, pp. 19–24.

[8] W. R. Broughton, M. J. Lodeiro, and G. D. Sims, “Validation of Procedures for ultrasonic C-scan Inspection of PMCs: UK Round-Robin,” NPL Report CMMT(A)179, 1999.

[9] K. F. Karlsson and T. B. Åström, “Manufacturing and applications of structural sandwich components,” *Compos. Part A Appl. Sci. Manuf.*, vol. 28, no. 2, pp. 97–111, 1997.

[10] C. Kyriazoglou and F. J. Guild, “Quantifying the effect of homogeneous and localized damage mechanisms on the damping properties of damaged GFRP and CFRP continuous and woven composite laminates-an FEA approach,” *Compos. Part A Appl. Sci. Manuf.*, vol. 36, no. 3, pp. 367–379, 2005.

Excerpt from ISBN 978-3-00-053387-7